MATHEMATICAL ANALYSIS OF A TUMOUR-IMMUNE INTERACTION MODEL: A MOVING BOUNDARY PROBLEM

JOSEPH MALINZI*

Department of Mathematics and Applied Mathematics, University of Pretoria
Private Bag X 20, Hatfield, Pretoria 0028, South Africa
Department of Mathematics, University of Eswatini, Private Bag 4, Kwaluseni, Eswatini

INNOCENTER AMIMA

Department of Mathematical Sciences, Stellenbosch University
Private Bag X1 Matieland, 7602, South Africa

ABSTRACT. A spatio-temporal mathematical model, in the form of a moving boundary problem, to explain cancer dormancy is developed. Analysis of the model is carried out for both temporal and spatio-temporal cases. Stability analysis and numerical simulations of the temporal model replicate experimental observations of immune-induced tumour dormancy. Travelling wave solutions of the spatio-temporal model are determined using the hyperbolic tangent method and minimum wave speeds of invasion are calculated. Travelling wave analysis depicts that cell invasion dynamics are mainly driven by their motion and growth rates. A stability analysis of the spatio-temporal model shows a possibility of dynamical stabilization of the tumour-free steady state. Simulation results reveal that the tumour swells to a dormant level.

1. **Introduction.** Research indicates that patients who have been treated for cancer can still have circulating disseminating tumour cells 10 to 20 years later [1–4]. These circulating tumour cells are either induced to a dormant state by its interaction with immune cells or progress to become more aggressive tumours [1, 3]. The dormant tumour cells appear and function like normal cells and over the years these cells develop active drug resistance that protects them from responding to treatment [5]. The host's immune system is known to defend the body from any invading pathogens such as virus or bacteria [6] and in some cases tumour cells [7–9]. Therefore, a lot of theoretical and experimental research is being carried out to understand and investigate the interactions between growing tumours and the immune system. However, it is hard to experimentally control the dynamics of tumour cells as they change continuously. Further, tumour cells develop mechanisms of suppressing anti-tumour activities [7–9].

The avascular stage which is the early stage of tumour formation happens in the absence of a vascular network. The transition from the avascular stage to vascular stage depends on the ability of the tumour to induce new blood vessels which eventually penetrate into the tumour to obtain blood supply, oxygen supply and micro-circulation [10]. The avascular stage can last up to several years due to competition among tumour

2010 *Mathematics Subject Classification.* Primary: 35R37 , 92D25; Secondary: 49K20 .

Key words and phrases. moving boundary problem, cancer dormancy, tumour-immune interactions, travelling wave solutions, hyperbolic tangent method, tumour radius.

* Corresponding author: Joseph Malinzi.

cells for metabolites or the competition between immune cells and tumour cells for metabolites and space [10]. The avascular stage is characterized by chronic inflammatory infiltrations of T-lymphocytes, B-lymphocytes, Natural-Killer (NK) cells, basophils, eosinophils and neutrophils [7, 11]. The tumour secretes soluble diffusible factors into the surrounding tissues and this enables these cells to penetrate the interior of the tumour [12, 13]. These factors are called chemokines and the immune cells migration is mostly driven by diffusion and chemotaxis in response to the presence of chemokines. The migrated immune cells interact with the growing tumour cells to form tumour-immune complexes which results in either the death of tumour cells or inactivation of immune cells [12, 13].

Avascular tumours can be effectively controlled by tumour infiltrating cytotoxic lymphocytes (TICLs) [14, 15]. The T-cells respond to the presence of a tumour since it provokes an immune response depending on the antigenicity. If it is high, then the tumour provokes a large immune response and the T-cells would eradicate the tumour. The TICLs may be cytotoxic lymphocytes (CTLs, CD8+ cells), natural killer-like (NK-like) cells or lymphokine activated killer (LAK) cells [11]. In this article, we refer to the TICLs as immune cells.

In spite of the progress made in investigating the mechanisms of interaction between tumour cells with immune cells, much is still unknown about the dynamics of tumour-immune interactions to explain cancer dormancy, a situation when tumour cells remain quiescent for a long time period [3, 16]. Lack of information on the mechanisms of cancer dormancy and the active mechanisms during cancer dormancy has been a major shortcoming in understanding the full complexes of metastatic growth [3, 16–18]. The complexity of tumour-immune interactions requires more research to capture more realistic dynamics of the essential biology [19]. Mathematical models and analysis, for example [18–25, 38], can therefore be used to explain complex natural phenomena like cancer dormancy.

As far as mathematical studies on tumour-immune interactions in line with cancer dormancy are concerned, several models have been constructed and analysed using deterministic approaches, for example [19, 20, 23–25], stochastic methods, e.g. [26–28] and of recent using kinetic models stemming from theories of statistical mechanics, for example [29]. We briefly review some mathematical studies on tumour-immune dynamics on which some of the aspects are most essential to this study. Extensive reviews on mathematical models of tumour-immune dynamics in relation to cancer dormancy can be found in [30–32].

Matzavinos *et al*. [18] presented a model to investigate the spatio-temporal dynamics of a tumour in the presence of an immune response. The study focussed on the interaction between TICLs and a multicellular immunogenic tumour which was at some stage prior to tumour-induced angiogenesis. Further, the study determined critical parameter values for cancer cells to exist in the body but remain in a clinically undetectable threshold for years to decades [17]. It was shown that the behaviour of the system was determined by crucial parameters such as the rate of binding immune cells with cancer cells, the chemotaxis of immune cells in response to the presence of chemokines and the probability of inactivating the immune cell after its interaction with a tumour cell.

Mallet and de Pillis [21] presented a spatio-temporal mathematical model to describe the immune response to a tumour growing in proximity of a nutrient source. Their model considered the dynamics of the tumour with both the TICLs and NK cells. Their analysis replicated the proliferation of the outer band of a tumour and the creation of a necrotic core at the centre in the absence of the immune system. It was shown

that the morphology of the tumour in response to immune cells depends on the choice of immune cells' recruitment and death. For almost all other immune cell parameters, resulted into osculations in the tumour and immune concentrations. Further, they noted that the immune cells had the ability of destroying the tumour depending on the TICLs recruitment and death rates although the tumour could as well grow in a stable or unstable oscillatory manner.

de Pillis et al. [22] in a follow up of the work of Mallet and de Pillis [21] examined four mechanisms that can likely determine the morphological structure of a growing tumour. Among these, was the response of different immune cell levels and induction strengths to the tumour. They investigated the mechanisms by simulating an extended model version of that in [21]. They showed that the immune cells were capable of decreasing a tumour to a small size, although it could return to a second growth phase hence evading the immune system control. It was further shown, just like in [21], that a stronger recruitment of immune cells induces a fast and more effective response to the tumour and thus reducing it to a small size or even destroying it. However, a small initial immune recruitment would eventually result into the tumour growing unboundedly. They further observed that, in the case of a high immune recruitment rate, the immune cells appeared to surround and lyse tumour cells.

One essential aspect of tumour growth is that its morphology keeps changing over time [33, 34]. Tumour growth as a free boundary has extensively been studied and partial differential equation models to describe tumour radius growth have been formulated [33–35]. These models are based on the principle of mass conservation and reaction diffusion in the tumour [33]. Greenspan [33] proposed a simple mathematical model of tumour growth in terms of diffusion of nutrients from sorrounding body tissue to the tumour. He assumed that the shape of a tumour is spherically symmetric and applied the mass conservation principle. Friedman [34] gave a brief review of free boundary tumour growth models and provided a methodical guide to the increasing number of models.

Tumour structure and geometry is highly intricate [18, 25, 34]. It is therefore imperative to extend existing tumour-immune models to account for a more realistic tumour geometry. In the present paper we pick up on the growing literature of spatio-temporal mathematical models to investigate tumour dormancy. The main goal here is to investigate tumour dormancy by constructing and analysing a moving boundary problem, that is, with a consideration of the tumour radius as a function of time rather than considering it to be constant as assumed in the literature of tumour-immune models before. The model we construct considers a simplified process of a growing avascular tumour that stimulates an immune response. Mathematical and numerical analyses are performed to investigate the mechanisms of tumour-immune interactions to explain tumour dormancy. Our objective is to (a) estimate the tumour radius with time, (b) examine critical parameters that promote tumour dormancy and (c) analyse the spatial distribution associated with an immune response to the presence of cancer cells by for example determining analytical travelling wave solutions.

2. **The model.**

The model we construct describes the growth of an avascular tumour, in a spherical geometric setting under radial symmetry, with radius $R(t)$ which is time dependent.

2.1. **Model assumptions and formulation.**

The following assumptions are made in constructing the model:

(1) Propagation dynamics of the tumour and immune cells are described using logistic growth functions [18, 21, 22].
(2) Both immune and tumour cells diffuse in body tissue [18, 21, 22].
(3) Proliferation of immune cells due to the presence of tumour cells is of Michaelis-Menten form [36, 37]. The term has been previously considered by some recent models, for example, [25, 38] to indicate the saturation effects of an immune response [39].
(4) The inactivated immune cells are quickly eliminated as they are produced. These cells do not have an effect on any other variables in the system and the focus here is on tumour-immune interactions [38].
(5) Chemokines are produced when lymphocytes are activated by tumour-immune interactions [12, 13]. Thus chemokine production is proportional to the cell complex density [18].
(6) The volume of extracellular space in tumours is approximately between 25% — 65% of the total volume of cells therefore, there is no competition for space between immune and tumour cells [40].

At every given value of time t and space r, there exists four cell densities, a chemokine concentration and a tumour radius: (i) $X(t,r)$: immune cells density in cells cm^{-3}, (ii) $Y(t,r)$: tumour cell density in cells cm^{-3}, (iii) $X^*(t)$: density of inactivated immune cells in cells cm^{-3}, (iv) $Y^*(t)$: density of dead tumour cells in cells cm^{-3}, (v) $U(t,r)$: chemokine concentration in cells cm^{-3} and (vi) $R(t)$: tumour radius in cm.

The interactions between the tumour and immune cells are represented by the schematic diagram in Figure 1.

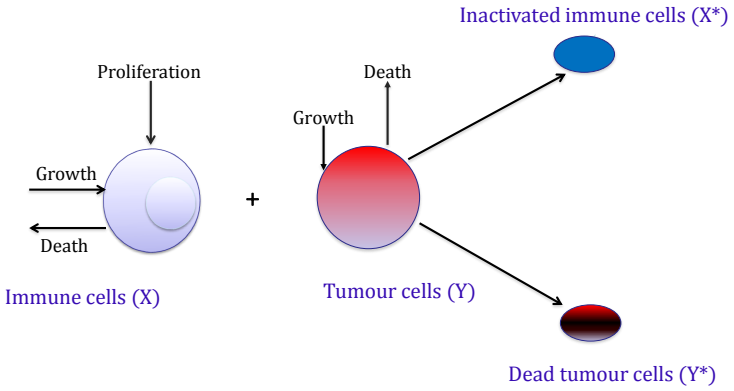

FIGURE 1. **A schematic diagram showing tumour-immune interactions. The interactions lead to the death of tumour cells or inactivation of immune cells.**

A logistic growth function is used to describe the growth dynamics of immune cells, together with a proliferation term and the local kinetic interactions shown in Figure 1.

On top of the immune cells moving randomly, their movement is also directed by the chemokine concentration secreted upon coming into contact with tumour cells. They move in the direction opposite to the chemokine gradient, that is, towards a region with a high chemokine concentration. Tumour growth is also assumed to progress logistically and its interaction with immune cells is modelled by the local kinetic terms derived in Matzavinos *et al.* [18]. Tumour-immune interactions can result in either the death of tumour cells Y^* or the inactivation of immune cells X^*. Immune and tumour cells compete in a predator-prey fashion [41].

Going by the above assumptions we consider the following moving boundary problem:

$$
\begin{aligned}
\frac{\partial X}{\partial t} &= \underbrace{\frac{\psi_X}{r^2}\frac{\partial}{\partial r}\left(r^2\frac{\partial X}{\partial r}\right)}_{\text{diffusion}} \underbrace{-\beta X\frac{1}{r^2}\frac{\partial}{\partial r}\left(r^2\frac{\partial U}{\partial r}\right)-\beta\frac{\partial X}{\partial r}\frac{\partial U}{\partial r}}_{\text{chemotaxis}} + \underbrace{\alpha_1 X(1-\alpha_2 X)}_{\text{logistic growth}} + \underbrace{\frac{fXY}{\gamma+Y}}_{\text{proliferation}} \\
&\quad \underbrace{-\phi_1 XY,}_{\text{immune inactivation}} \quad 0 \le r \le R(t) \\
\frac{\partial Y}{\partial t} &= \underbrace{\frac{\psi_Y}{r^2}\frac{\partial}{\partial r}\left(r^2\frac{\partial Y}{\partial r}\right)}_{\text{diffusion}} + \underbrace{\beta_1 Y(1-\beta_2 Y)}_{\text{logistic growth}} \underbrace{-\phi_2 XY,}_{\text{tumour lysis}} \quad 0 \le r \le R(t) \\
\frac{\partial U}{\partial t} &= \underbrace{\frac{\psi_U}{r^2}\frac{\partial}{\partial r}\left(r^2\frac{\partial U}{\partial r}\right)}_{\text{diffusion}} + \underbrace{\phi_3 XY}_{\text{production}} \underbrace{-d_1 U,}_{\text{decay}} \\
\frac{\partial X^*}{\partial t} &= \underbrace{\phi_1 XY}_{\text{formation of } X^*} \underbrace{-d_2 X^*,}_{\text{decay}} \\
\frac{\partial Y^*}{\partial t} &= \underbrace{\phi_2 XY}_{\text{formation of Y*}} \underbrace{-d_3 Y^*,}_{\text{decay}} 0 \le r \le R(t)
\end{aligned}
\tag{1}
$$

The term $\frac{\psi_X}{r^2}\frac{\partial}{\partial r}\left(r^2\frac{\partial X}{\partial r}\right)$ represents random movement of immune cells where ψ_X is immune cells' diffusivity. Directed movement of immune cells via the chemokine gradient is described by the term $-\beta X\frac{1}{r^2}\frac{\partial}{\partial r}\left(r^2\frac{\partial U}{\partial r}\right)-\beta\frac{\partial X}{\partial r}\frac{\partial U}{\partial r}$, where β is a chemotaxis constant. The expression $\alpha_1 X(1-\alpha_2 X)$ describes immune cells propagation, where α_1 and $1/\alpha_2$ are respectively the intrinsic growth rate and the carrying capacity of immune cells. The expression $fXY/(\gamma+Y)$ describes immune cells proliferation where f is the multiplication rate. The Michaelis constant γ represents the tumour concentration when the immune density is half-maximal. The term $-\phi_1 XY$ represents a proportion of deactivated immune cells as a result of interacting with tumour cells where ϕ_1 is the rate of deactivation. The term $\frac{\psi_Y}{r^2}\frac{\partial}{\partial r}\left(r^2\frac{\partial Y}{\partial r}\right)$ represents tumour cells diffusion where ψ_Y is tumour cells' diffusivity. $\beta_1 Y(1-\beta_2 Y)$ represents tumour growth where β_1 and $1/\beta_2$ cells cm^{-3} are respectively the intrinsic growth rate and the carrying capacity of the tumour cells. The expression $-\phi_2 XY$ describes the proportion of dead tumour cells as a result of their interaction with immune cells where ϕ_2 is the lysis rate of tumour cells by immune cells. The term $\frac{\psi_U}{r^2}\frac{\partial}{\partial r}\left(r^2\frac{\partial U}{\partial r}\right)$ represents chemokine diffusion, where ψ_U is the chemokine diffusion constant. $\phi_3 XY$ describes chemokine production and $d_1 U$ describes its decay where ϕ_3 is the rate of chemokine production and d_1 is the rate of decay measured per day. The formation of inactivated immune cells and dead tumour cells is respectively represented by $\phi_1 XY$ and $\phi_2 XY$. The parameters d_2 and

d_3 denote the rate of decay of the inactivated immune cells and the dead tumour cells respectively. The fourth equation in (1) has no effect on the rest of the system and our aim is to study tumour-immune interactions. It therefore suffices to ignore it for the rest of this study.

2.2. **Derivation of tumour radius.** The tumour is assumed to be spherical with radius $R(t)$. To generate an equation for the tumour radius with time, the total tumour mass inside the sphere is determined by firstly integrating the sum of the second and last equations in (1) over the solid spherical volume as

$$\begin{aligned}\int_0^{R(t)} r^2\left(\frac{\partial Y}{\partial t}+\frac{\partial Y^*}{\partial t}\right)dr &= \int_0^{R(t)} -\frac{\partial(1-Y)}{\partial t}r^2dr+\int_0^{R(t)} -\frac{\partial(1-Y^*)}{\partial t}r^2dr\\ &= \psi_Y\int_0^{R(t)}\frac{\partial}{\partial r}\left(r^2\frac{\partial Y}{\partial r}\right)dr+\int_0^{R(t)} r^2(\beta_1 Y(1-\beta_2 Y)-d_3Y^*)\,dr.\end{aligned} \tag{2}$$

Let the total tumour density $Y+Y^*=T$. By using Leibniz's rule, the left hand side of Equation (2) becomes:

$$\begin{aligned}\int_0^{R(t)} -\frac{\partial(1-Y)}{\partial t}r^2dr+\int_0^{R(t)} -\frac{\partial(1-Y^*)}{\partial t}r^2dr &= -\int_0^{R(t)}\frac{\partial(1-T)}{\partial t}r^2dr\\ &= -\frac{d}{dt}\int_0^{R(t)}(1-T)r^2dr+(1-T_1)R^2\frac{dR}{dt},\end{aligned}$$

where $T_1=T(t,R(t))\neq 1$. By evaluating the spatial integral, the right hand side of Equation (2) becomes:

$$\begin{aligned}\psi_Y\int_0^{R(t)}\frac{\partial}{\partial r}\left(r^2\frac{\partial Y}{\partial r}\right)dr+\int_0^{R(t)} r^2(\beta_1 Y(1-\beta_2 Y)-d_3Y^*)\,dr &\\ = \psi_Y R^2\frac{\partial Y}{\partial r}(t,R(t))+\int_0^{R(t)} r^2(\beta_1 Y(1-\beta_2 Y)-d_3Y^*)\,dr.&\end{aligned}$$

Therefore,

$$\begin{aligned}-\frac{d}{dt}\int_0^{R(t)}(1-T)r^2dr+(1-T_1)R^2\frac{dR}{dt} &\\ = \psi_Y R^2\frac{\partial Y}{\partial r}[t,R(t)]+\int_0^{R(t)} r^2(\beta_1 Y(1-\beta_2 Y)-d_3Y^*)\,dr.&\end{aligned}$$

Noting that $\frac{\partial Y}{\partial r}(t,R(t))=0$, the tumour radius is found to obey the equation

$$R^2\frac{dR}{dt}=\frac{1}{1-T_1}\int_0^{R(t)} r^2(\beta_1 Y(1-\beta_2 Y)-d_3Y^*)\,dr+\frac{1}{1-T_1}\frac{d}{dt}\int_0^{R(t)}(1-T)r^2dr. \tag{3}$$

2.3. **Boundary and initial conditions.** The choice of boundary conditions is influenced by the assumption that we consider an avascular tumour and therefore cells do not escape from the tissue membranes in which they are initially contained. We therefore consider the following zero-flux boundary conditions for the immune and tumour cells, and chemokine concentration

$$\boldsymbol{n}\cdot\nabla X=\boldsymbol{n}\cdot\nabla Y=\boldsymbol{n}\cdot\nabla U=0. \tag{4}$$

where $\boldsymbol{n}$ is a normal to the vectors X, Y and U. Initially, we consider that the tumour occupies a bigger part of the domain and that immune cells occupy more of the region towards the sheath of the tumour, that is, near $r = 0$ and $r = 1$. The initial tumour and immune cell densities are therefore taken to be Gaussian profiles just like in [42, 43]. We consider constant initial concentrations for the chemokine concentration and dead tumour cells.

$$\begin{aligned} X(0,r) &= X_0 e^{\frac{1}{2}(x-0.5)^2}, \quad 0 \le r \le 1, \\ Y(0,r) &= Y_0 e^{-\frac{1}{2}\left(\frac{x-0.5}{0.1}\right)^2}, \quad 0 \le r \le 1, \\ U(0,r) &= U_0, \quad 0 \le r \le 1, \\ Y^*(0) &= Y_0^*,\ X^*(0) = X_0^*,\ R(0) = R_0. \end{aligned} \tag{5}$$

2.4. **Model re-scaling and boundary transformation.** We use the Landau [44] boundary fixing transformation

$$\bar{r} = \frac{r}{R(t)} \tag{6}$$

so that $0 \le r < R(t)$ is mapped to $0 \le \bar{r} < 1$. The model variables are rescaled by defining new variables in terms of their initial concentrations $x = X/X_0$, $y = Y/Y_0$, $y^* = Y^*/Y_0^*$, $u = U/U_0$, $\bar{R} = R/R_0$, $\bar{t} = t/t_0$, $\bar{r} = r/r_0$ where $t_0 = d_1^{-1}$ and r_0 is taken to be 1. The parameters become:

$$\psi_x = \frac{\psi_X t_0}{R_0^2}, \quad \bar{\beta} = \frac{\beta t_0}{R_0^2}, \quad \psi_y = \frac{\psi_Y t_0}{R_0^2}, \quad \psi_u = \frac{\psi_U t_0}{R_0^2}, \quad \varphi_1 = \alpha_1 t_0, \quad \varphi_2 = \alpha_2 X_0,$$
$$\delta = f_1 t_0, \quad \bar{\gamma} = \frac{\gamma}{Y_0}, \quad \nu_1 = \phi_1 Y_0 t_0, \quad \sigma_1 = \beta_1 t_0, \quad \sigma_2 = \beta_2 X_0, \quad \nu_2 = \phi_2 X_0 t_0,$$
$$\mu_1 = d_1 t_0, \quad \rho = \frac{\phi_2 X_0 Y_0 t_0}{Y_0^*}, \quad \nu_3 = \frac{\phi_3 X_0 Y_0 t_0}{U_0}, \quad \mu_2 = d_3 t_0.$$

Dropping the bars for simplicity gives the following rescaled system:

$$\begin{aligned} \frac{\partial x}{\partial t} &= \frac{\psi_x}{R(t)^2}\left(\frac{\partial^2 x}{\partial r^2} + \frac{2}{r}\frac{\partial x}{\partial r}\right) - \frac{\beta}{R(t)^2}\left(x\frac{\partial^2 u}{\partial r^2} + \frac{2x}{r}\frac{\partial y}{\partial r} + \frac{\partial u}{\partial r}\frac{\partial x}{\partial r}\right) \\ &\quad + \varphi_1 x(1-\varphi_2 x) + \frac{\delta x y}{\gamma + y} - \nu_1 x y, \\ \frac{\partial y}{\partial t} &= \frac{\psi_y}{R(t)^2}\left(\frac{\partial^2 y}{\partial r^2} + \frac{2}{r}\frac{\partial y}{\partial r}\right) + \sigma_1 y(1-\sigma_2 y) - \nu_2 x y, \\ \frac{\partial u}{\partial t} &= \frac{\psi_u}{R(t)^2}\left(\frac{\partial^2 u}{\partial r^2} + \frac{2}{r}\frac{\partial u}{\partial r}\right) + \nu_3 x y - \mu_1 u, \\ \frac{\partial y^*}{\partial t} &= \rho x y - \mu_2 y^*, \\ R^2\frac{dR}{dt} &= \frac{1}{1-\bar{T}_1}\int_0^{R(t)} r^2(\sigma_1 y(1-\sigma_2 y) - \mu_2 y^*)\,dr + \frac{1}{1-\bar{T}_1}\frac{d}{dt}\int_0^{R(t)}(1-\bar{T})r^2 dr, \end{aligned} \tag{7}$$

where $\bar{T} = y + y^*$ and $\bar{T}_1 = \bar{T}(t,1)$ with initial condition:

$$x(0,r) = x_0 e^{\frac{1}{2}(r-0.5)^2}, \ \ y(0,r) = y_0 e^{-\frac{1}{2}\left(\frac{r-0.5}{0.1}\right)^2}, \ \ u(0,r) = u_0, \ \ y^*(0) = y_0, \ \ \& \ R(0) = R_0 \tag{8}$$

and boundary conditions:

$$\frac{\partial x}{\partial r}(0,t)=\frac{\partial x}{\partial r}(1,t)=\frac{\partial x}{\partial r}(0,t)=\frac{\partial y}{\partial r}(1,t)=\frac{\partial u}{\partial r}(0,t)=\frac{\partial u}{\partial r}(1,t)=0. \tag{9}$$

3. **Temporal model analysis.** In this section, the temporal model phase space properties are investigated and a stability analysis of its steady state solutions is carried out. Without the consideration of space, that is, all model variables are independent of r and assuming that

$$\frac{d}{dt}\int_0^{R(t)}(1-T)r^2dr=0,$$

the tumour radius is given by

$$\frac{dR}{dt}=\frac{R}{3[1-(y+y^*)]}\Big[\sigma_1 y(1-\sigma_2 y)-\mu_2 y^*\Big]. \tag{10}$$

Model (7) is transformed to the following system of differential equations:

$$\begin{aligned}
\frac{dx}{dt}&=\varphi_1 x(1-\varphi_2 x)+\frac{\delta xy}{\gamma+y}-\nu_1 xy,\\
\frac{dy}{dt}&=\sigma_1 y(1-\sigma_2 y)-\nu_2 xy,\\
\frac{du}{dt}&=\nu_3 xy-\mu_1 u,\\
\frac{dy^*}{dt}&=\rho xy-\mu_2 y^*,\\
\frac{dR}{dt}&=\frac{R}{3[1-(y+y^*)]}\Big[\sigma_1 y(1-\sigma_2 y)-\mu_2 y^*\Big].
\end{aligned} \tag{11}$$

3.1. **Solution properties.**

Theorem 3.1. *The following model solution properties are preserved:*

1. *The tumour-immune interaction Model (11) has a positive unique solution that exists and remains in some domain $\mathbb{D}=[0,b)$, $b>0$ for all $t\geqslant 0$ for positive initial conditions.*
2. *The solutions to the model (11) are bounded from above and the trajectories evolve in an attracting region Ω where*

$$\Omega=\Big\{(x,y,u,y^*,R)\in\mathbb{R}^5_+\mid 0<x\leq\frac{\varphi_1-A}{\varphi_1\varphi_2},\quad 0\leq y\leq\frac{1}{\sigma_2},\quad 0\leq u\leq\frac{B\nu_3}{\mu_1},$$
$$0\leq y^*\leq\frac{B\rho}{\mu_2},\quad 0<R\leq R^*\Big\},$$

$$A=\frac{\nu_1}{\sigma_2},B=\frac{\varphi_1-A}{\varphi_1\varphi_2\sigma_2}\ \text{and}\ R^*=R_0\exp\Big(T\max_{0\leq t\leq T}\phi(s)\Big).$$

Proof of Theorem 3.1. 1. We use Theorem **A.4.** in [45] to prove existence and positivity. It is stated as follows: *Let $\mathbb{R}^n_+=[0,\infty)$ be the cone of non-negative vectors in $\mathbb{R}^n$. Let $F:\mathbb{R}^{n+1}_+\to\mathbb{R}^n$ be locally Lipschitz,*

$$F(t,x)=(F_1(t,x),\cdots F_n(t,x)),\quad x=(x_1,\cdots x_n),$$

and satisfy

$$F_j(t,x)\geq 0\ \text{whenever}\ t\geq 0,\ x\in\mathbb{R}^n_+,\ x_j=0. \tag{12}$$

Then, for every $x^\circ \in \mathbb{R}^n_+$, there exists a unique solution of $x' = F(t,x)$, $x(0) = x^\circ$, with values in $\mathbb{R}^n_+$, defined on some interval $[0,b)$, $b>0$.
The functions, $F(x,y,u,y^*,R)$, on the left of Equations (11) and their partial derivatives are continuous on $\mathbb{R}_+$ and the conditions in Equation (12) are satisfied.

2. From Equation (11)

$$\frac{dy}{dt} = \sigma_1 y(1-\sigma_2 y) - \nu_2 xy \leqslant \sigma_1 y(1-\sigma_2 y) \text{ since } \nu_2,\, x,\, y \geqslant 0.$$

Let us consider

$$\frac{dP}{dt} = \sigma_1 P(1-\sigma_2 P) \text{ such that } P(t) \geqslant y(t) \text{ for all } t \in [0,\infty).$$

$$P(t) = \frac{P(0)}{\big(1-\sigma_2 P(0)\big)e^{(-\sigma_1 t)} + \sigma_2 P(0)}.$$

$$\lim_{t\to\infty} P(t) = \frac{1}{\sigma_2} \text{ which implies that } \limsup_{t\to\infty} y(t) = \frac{1}{\sigma_2}. \tag{13}$$

Using the upper bound for the tumour cells we can rewrite the rate of change in immune cell concentration as

$$\frac{dx}{dt} \leqslant \varphi_1 x(1-\varphi_2 x) - Ax.$$

Let

$$\frac{dS}{dt} = \varphi_1 S(1-\varphi_2 S) - AS \text{ such that } S(t) \geqslant x(t) \text{ for all } t \in [0,\infty).$$

$$S(t) = \frac{S(0)(\varphi_1 - A)}{\big(\varphi_1(1-\varphi_2 S(0)) - A\big)e^{(-t(\varphi_1 - A))} + \varphi_1\varphi_2 S(0)}.$$

$$\lim_{t\to\infty} S(t) = \frac{\varphi_1 - A}{\varphi_1\varphi_2} \text{ which implies } \limsup_{t\to\infty} x(t) = \frac{\varphi_1 - A}{\varphi_1\varphi_2}.$$

Similarly, the third and fourth equations of (11) can be written as

$$\frac{du}{dt} \leq B\nu_3 - \mu_1 u \text{ and } \frac{dy^*}{dt} \leq B\rho - \mu_2 y^*,$$

for which one has

$$u(t) \leq \frac{B\nu_3}{\mu_1} + \left(u_0 - \frac{B\nu_3}{\mu_1}\right)\exp(-\mu_1 t) \text{ and } y^*(t) \leq \frac{B\rho}{\mu_2} + \left(y_0^* - \frac{B\rho}{\mu_2}\right)\exp(-\mu_2 t)),$$

and consequently

$$\limsup_{t\to\infty} u(t) \leq \frac{B\nu_3}{\mu_1} \text{ and } \limsup_{t\to\infty} y^*(t) \leq \frac{B\rho}{\mu_2}. \tag{14}$$

Finally, the radius equation in (11) can be solved to give

$$R(t) = R_0 \exp \int_0^t \phi(s)ds, \quad 0 \leq t \leq T,$$

where

$$\phi(s) = \int_o^t \left(\frac{\sigma_1 y(s)(1-\sigma_2 y(s)) - \mu_2 y^*}{3[1-(y(s)+y^*(s))]}\right)ds.$$

This implies that

$$R^* = R_0 \exp\left(\int_0^T \max_{0\le t\le T}(\phi(s)ds)\right) = R_0 \exp\left(T \max_{0\le t\le T}\phi(s)\right).$$

□

Theorem 3.1 implies that for any finite time, the cell and chemokine concentrations and tumour radius are not only non-negative but also bounded. The tumour cells are bounded by their carrying capacity and the immune cells are bounded by a fraction of their carrying capacity. This indicates that the model solutions are biologically meaningful. Next, the long-term behaviour of the temporal model solutions is investigated by determining steady states and their stability.

3.2. **Steady state solutions and stability analysis.** Without the consideration of space, it is important to note that, the third to fifth equations in (11) do not affect the first two equations. That is to say, the chemokine, dead tumour cells and the tumour radius have no effect on the immune and tumour cells growth. Here, we are interested in the long term dynamics of the immune and tumour cells in (15). Nonetheless we later, while doing numerical simulations, estimate the tumour radius.

$$\begin{aligned}\frac{dx}{dt} &= \varphi_1 x(1-\varphi_2 x) + \frac{\delta xy}{\gamma_1 + y} - \nu_1 xy,\\ \frac{dy}{dt} &= \sigma_1 y(1-\sigma_2 y) - \nu_2 xy.\end{aligned} \tag{15}$$

The Model (15) has five steady states with only two being biologically well defined in the domain Ω. There are five states with three biologically meaningful ones, that is, X_2^*, X_4^* and X_5^*.

$$X_1^* := (x^*, y*) = (0,0), \quad X_2^* := (x^*, y*) = \left(\frac{1}{\varphi_2}, 0\right), \quad X_3^* := (x^*, y*) = \left(0, \frac{1}{\sigma_2}\right),$$

$$X_4^* := (x^*, y*) = \left(\frac{\varphi_1 + \frac{\delta y^*}{\kappa + y^*} - \nu_1 y^*}{\varphi_1\varphi_2}, \frac{-\omega_2 \pm \sqrt{\omega_2^2 - 4\omega_1\omega_3}}{2\omega_1}\right),$$

$$X_5^* := (x^*, y*) = \left(\frac{-\phi_2 \pm \sqrt{\phi_2^2 - 4\phi_1\phi_3}}{2\phi_1}, \frac{\sigma_1 - \nu_2 x^*}{\sigma_1\sigma_2}\right),$$

where

$$\omega_1 = \nu_1\nu_2 - \sigma_1\sigma_2\varphi_1\varphi_2, \qquad \omega_2 = \varphi_1\varphi_2\sigma_1 - \kappa\varphi_1\varphi_2\sigma_1\sigma_2 - \varphi_1\nu_2 - \delta\nu_2 + \kappa\nu_1\nu_2,$$
$$\omega_3 = \kappa\varphi_1\varphi_2\sigma_1 - \kappa\varphi_1\nu_2, \qquad \phi_1 = \varphi_1\varphi_2\nu_2,$$
$$\phi_2 = -\sigma_1\sigma_2\varphi_1\varphi_2\kappa - \varphi_1\nu_2 - \varphi_1\varphi_2\sigma_1 - \delta\nu_2 + \frac{\kappa\nu_1\nu_2}{\varphi_1\varphi_2} + \frac{2\sigma_1\nu_1\nu_2}{\varphi_1\varphi_2\sigma_1\sigma_2},$$
$$\phi_3 = \kappa\varphi_1\sigma_1\sigma_2 + \varphi_1\sigma_1 + \delta\sigma_1 - (\kappa\nu_1\sigma_1)/(\varphi_1\varphi_2) - \frac{\sigma_1^2\nu_1}{\sigma_1\sigma_2\varphi_1\varphi_2}.$$

At any given time body tissue should at least contain immune cells. This makes the trivial steady state X_1^* and X_3^* biologically unrealistic. The fifth steady state, X_5^*, is not biologically meaningful because $\sigma_1 - \nu_2 x^* < 0$. This makes X_2^* and X_4^* the only biologically meaningful steady states.

Next, stability analysis of the tumour-free state X_2^* and the tumour-dormant state X_4^* is investigated.

Proposition 1. *The tumour-free state X_2^* is asymptotically stable if $\sigma_1 < \nu_2/\varphi_2$ and unstable otherwise.*

Proof of Theorem 1. The Jacobian matrix for the tumour-free state X_2^* is

$$DF(X_2^*) = \begin{pmatrix} -\varphi_1 & \frac{\delta}{\varphi_2\gamma_1} - \frac{\nu_1}{\varphi_2} \\ 0 & \sigma_1 - \frac{\nu_2}{\varphi_2} \end{pmatrix}, \quad \text{with eigenvalues} \quad -\varphi_1 \quad \text{and} \quad \sigma_1 - \frac{\nu_2}{\varphi_2}.$$

□

Proposition 2. *If $\sigma_1 \geq \nu_2/\varphi_2$, the tumour-dormant state X_4^* is globally stable for the feasible parameter values in Table 1.*

Proof of Theorem 2. Suppose a positive definite Lyapunov function candidate is defined by $V(X) = Ax^2 + By^2$, $A, B > 0$. The rate of change of $V(X)$ at the tumour-dormant state X_4^* is given as

$$\begin{aligned} \frac{dV(\boldsymbol{X}_4^*)}{dt} &= \begin{bmatrix} \frac{\partial V}{\partial x} & \frac{\partial V}{\partial y} \end{bmatrix} \begin{bmatrix} f_1(t, x^*, y^*) \\ f_2(t, x^*, y^*) \end{bmatrix}, \\ &= \begin{bmatrix} 2Ax^* & 2By^* \end{bmatrix} \begin{bmatrix} \varphi_1 x^*(1 - \varphi_2 x^*) + \frac{\delta x^* y^*}{\kappa + y^*} - \nu_1 x^* y^* \\ \sigma_1 y^*(1 - \sigma_2 y^*) - \nu_2 x^* y^* \end{bmatrix}. \end{aligned}$$

Substituting the non-dimensional parameter values derived from Table 1 into the first derivative of the lyapunov function $\frac{dV(\boldsymbol{X}_4^*)}{dt}$ gives

$$\dot{V}(X_4^*) = -(3.296A + 0.0023B) < 0 \quad \text{for all } t.$$

This proves that the tumour-dormant state X_4^* is globally stable. Possibly this may be the same reason why a person can live with tumour cells for their entire life time without clinically detecting them.

□

4. Spatio-temporal model analysis.

Travelling wave solutions describe invasion dynamics and the parameters involved in wave solutions are therefore highly critical in determining the future cell densities in this case. In calculating the minimum wave speeds, we seek to determine the critical parameters which describe the potential with which cell densities invade each other.

4.1. Travelling wave analysis.

A special type of exact solutions to the Model (7) are determined on a fixed domain in one dimension (1D). That is, radius not dependent on time ($r \neq R(t)$). The hyperbolic tangent method is used to determine these solutions [46–48].

Travelling wave solutions. In order to determine the travelling wave solutions admitted by (7), we consider waves moving from the left to right with a wave number c and speed $\nu \neq c$. By letting $z = c(r - \nu t)$, Equations (7) (1-3) are transformed to

$$\begin{aligned} c\nu\frac{dx}{dz} + \psi_x c^2\frac{d^2x}{dz^2} - \beta c^2\left(x\frac{d^2u}{dz^2} + \frac{du}{dz}\frac{dx}{dz}\right) + \varphi_1 x(1 - \varphi_2 x) + \frac{\delta xy}{\gamma + y} - \nu_1 xy = 0, \\ c\nu\frac{dy}{dz} + \psi_y c^2\frac{d^2y}{dz^2} + \sigma_1 y(1 - \sigma_2 y) - \nu_2 xy = 0, \\ c\nu\frac{du}{dz} + \psi_u c^2\frac{d^2u}{dz^2} + \nu_3 xy - \mu_1 u = 0 \end{aligned} \tag{16}$$

with boundary conditions:

$$\lim_{t\to-\infty}(x,y,u)=X^0 \quad \text{and} \quad \lim_{t\to-\infty}(x,y,u)=X^1$$

where $X^0=(0,0,0)$ or $X^0=(1/\varphi_2,0,0)$ and $X^1:=(x^*,y^*,u^*)$ is the tumour endemic state.

Theorem 4.1. *The equations* (16) *exhibit closed form solutions of the form:*

$$x(t,r)=\frac{1}{4\varphi_2}\Big(1-\tanh\big(c(r-\nu t)\big)\Big)^2, \text{ where } c=\frac{1}{2\sqrt{6}}\sqrt{\frac{\varphi_1}{\psi_x}} \text{ and } \nu=\frac{5}{\sqrt{6}}\sqrt{\varphi_1\psi_x}$$

and

$$y(t,r)=\frac{1}{4\sigma_2}\Big(1-\tanh\big(c(r-\nu t)\big)\Big)^2, \text{ where } c=\frac{1}{2\sqrt{6}}\sqrt{\frac{\sigma_1}{\psi_y}} \text{ and } \nu=\frac{5}{\sqrt{6}}\sqrt{\sigma_1\psi_y}.$$

Proof. Using the hyperbolic tangent method, the following transformations are introduced:

$$\begin{aligned} W&=\tanh(z),\\ x(W)=F_1(W)&=(1-W)^{p_1}(1+W)^{q_1}\sum_{i=0}^{N-p_1-q_1}a_iW^n,\\ y(W)=F_2(W)&=(1-W)^{p_2}(1+W)^{q_2}\sum_{i=0}^{N-p_2-q_2}b_iW^n,\\ u(W)=F_3(W)&=(1-W)^{p_3}(1+W)^{q_3}\sum_{i=0}^{N-p_3-q_3}c_iW^n, \end{aligned} \tag{17}$$

where $p_1+q_1=2,3,\cdots,N$, $p_2+q_2=2,3,\cdots,N$, $p_3+q_3=2,3,\cdots,N$.

Equations (16) become

$$\begin{aligned} c\nu(1-W^2)\frac{dF_1}{dW}+\psi_x c^2(1-W^2)\frac{d}{dW}\Big((1-W^2)\frac{dF_1}{dW}\Big)\\ -\beta c^2F_1(W)(1-W^2)\frac{d}{dW}\Big((1-W^2)\frac{dF_3}{dW}\Big)-\beta c^2\Big(c^2\nu^2(1-W^2)^2\frac{dF_1}{dW}\frac{dF_3}{dW}\Big)\\ +\varphi_1F_1(W)(1-\varphi_2F_1(W))+\frac{\delta F_1(W)F_2(W)}{\gamma+F_2(W)}-\nu_1F_1(W)F_2(W)=0,\\ c\nu(1-W^2)\frac{dF_2}{dW}+\psi_y c^2(1-W^2)\frac{d}{dW}\Big((1-W^2)\frac{dF_2}{dW}\Big)\\ +\sigma_1F_2(W)(1-\sigma_2F_2(W))-\nu_2F_1(W)F_2(W)=0,\\ c\nu(1-W^2)\frac{dF_3}{dW}+\psi_u c^2(1-W^2)\frac{d}{dW}\Big((1-W^2)\frac{dF_3}{dW}\Big)+F_1(w)F_2(W)-\mu_1F_3(W)=0. \end{aligned} \tag{18}$$

The substitution of $F_i(W)$ in Equations (18) yields $p_i=q_i=1, i=1,2,3$, that is,

$$F_1(W)=a_0(1-W)^2, \quad F_2(W)=b_0(1-W)^2, \quad F_3(W)=c_0(1-W)^2. \tag{19}$$

The following results are obtained after substituting (19) into (18):

Either

$$a_0=\frac{1}{4\varphi_2}, \quad b_0=0, \quad c=\frac{1}{2\sqrt{6}}\sqrt{\frac{\varphi_1}{\psi_x}}, \quad \nu=\frac{5}{\sqrt{6}}\sqrt{\varphi_1\psi_x}, \quad c_0=0 \tag{20}$$

or

$$a_0 = 0, \quad b_0 = \frac{1}{4\sigma_2}, \quad c = \frac{1}{2\sqrt{6}}\sqrt{\frac{\sigma_1}{\psi_y}}, \quad \nu = \frac{5}{\sqrt{6}}\sqrt{\sigma_1\psi_y}, \quad c_0 = 0. \tag{21}$$

The results in Equations (20) and (21) respectively imply that the immune and tumour cells wave fronts are given by:

$$x(t,r) = \frac{1}{4\varphi_2}\Big(1-\tanh\big(c(r-\nu t)\big)\Big)^2, \text{ where } c = \frac{1}{2\sqrt{6}}\sqrt{\frac{\varphi_1}{\psi_x}} \text{ and } \nu = \frac{5}{\sqrt{6}}\sqrt{\varphi_1\psi_x}$$

and

$$y(t,r) = \frac{1}{4\sigma_2}\Big(1-\tanh\big(c(r-\nu t)\big)\Big)^2, \text{ where } c = \frac{1}{2\sqrt{6}}\sqrt{\frac{\sigma_1}{\psi_y}} \text{ and } \nu = \frac{5}{\sqrt{6}}\sqrt{\sigma_1\psi_y}.$$

□

Minimum wave speed.

Theorem 4.2. *The minimum wave speeds of invasion for the tumour and immune travelling wave fronts, respectively, are:*

$$\nu^y_{min} = 2\sqrt{\frac{\sigma_1\psi_y}{c^3}} \quad \textit{and} \quad \nu^x_{min} = 2\sqrt{\varphi_1\psi_x}. \tag{22}$$

Proof of Theorem 4.2. Equations (16) are transformed into first order differential equations by letting $y_1 = dx/dz$, $y_2 = dy/dz$, $y_3 = du/dz$ to get

$$\begin{aligned}
\frac{dy_1}{dt} &= \frac{1}{c^2\psi_x}\Big(\beta c^2(xy_3 + y_1y_3) - c\nu y_1 - \varphi_1 x(1-\varphi_2 x) - \frac{\delta xy}{\gamma+y} + \nu_1 xy\Big),\\
\frac{dx}{dt} &= x_1,\\
\frac{dy_2}{dt} &= \frac{1}{c^2\psi_y}\Big(-c\nu y_2 - \sigma_1 y(1-\sigma_2) + \nu_2 xy)\Big),\\
\frac{dy}{dt} &= y_2,\\
\frac{dy_3}{dt} &= \frac{1}{c^2\psi_u}\Big(-c\nu y_3 - \nu_3 xy + \mu_1 u\Big),\\
\frac{du}{dz} &= y_3.
\end{aligned} \tag{23}$$

The travelling wave solutions are trajectories connecting equilibrium X^0 to X^1. The trajectory leaving X^0 is therefore not required to oscillate, that is, the eigenvalues of the Jacobian matrix of (23) evaluated at X^0 must not have complex roots. The minimum wave speeds are thus determined by evaluating the eigenvalues of the Jacobian matrix (24) at X^0.

$$J(X^0) = \begin{pmatrix}
\frac{\nu}{(-\psi_x)c} & \frac{\psi_1}{(-\psi_x)c^2} & 0 & 0 & 0 & 0\\
1 & 0 & 0 & 0 & 0 & 0\\
0 & 0 & -\frac{c^3\nu}{\psi_y} & -\frac{c^2\sigma_1}{\psi_y} & 0 & 0\\
0 & 0 & 1 & 0 & 0 & 0\\
0 & 0 & 0 & 0 & -\frac{c^3\nu}{\psi_u} & \frac{c^2\mu_1}{\psi_u}\\
0 & 0 & 0 & 0 & 1 & 0
\end{pmatrix}. \tag{24}$$

The eigenvalues are:

$$-\frac{c^3\nu+\sqrt{c^4\nu^2-4\psi_y\sigma_1}c}{2\psi_y},-\frac{c^3\nu-\sqrt{c^4\nu^2-4\psi_y\sigma_1}c}{2\psi_y},\frac{\nu-\sqrt{-4\psi_1\psi_x+\nu^2}}{22\psi_x},$$
$$\frac{\nu+\sqrt{-4\psi_1\psi_x+\nu^2}}{22\psi_x},-\frac{c^3\nu+\sqrt{c^4\nu^2+4\mu_1\psi_u}c}{2\psi_u},-\frac{c^3\nu-\sqrt{c^4\nu^2+4\mu_1\psi_u}c}{2\psi_u}. \tag{25}$$

The conditions

$$\sqrt{c^4\nu^2-4\psi_y\sigma_1}c \quad \text{and} \quad \sqrt{-4\psi_1\psi_x+\nu^2} \tag{26}$$

must determine the minimum wave speed since all the other eigenvalues are real except for those with these terms. That is $c^4\nu^2-4\psi_y\sigma_1\geq 0$ and $-4\psi_1\psi_x+\nu^2\geq 0$ which gives

$$\nu^y_{\min}=2\sqrt{\frac{\sigma_1\psi_y}{c^3}} \quad \text{and} \quad \nu^x_{\min}=2\sqrt{\varphi_1\psi_x}.$$

□

Both the travelling wave solutions in Equations (20) & (21) and the minimum wave speeds in Equation (22) are characterized by the cell carrying capacities, diffusion constants. This implies that the cell invasion dynamics are mainly driven by their motion and growth rates. Treatment options should therefore strive to improve immune recognition of tumour cells, reduce the intrinsic growth rate of tumour cells and increase that for immune cells.

4.2. **Turing instability analysis.** We determine conditions for the formation of Turing patterns by perturbing the stable tumour-dormant state with small heterogeneous perturbations [49,50]. It is important to note that, for simplicity, Turing instability analysis was carried out for the model without chemotaxis (i.e $\beta\nabla\cdot(X.\nabla U)=0$) and on a fixed domain (i.e with the radius not depending on time). To investigate the influence of the presence of diffusion terms on the temporal system, consider a small perturbation $[\delta x,\delta y]$ to the steady state $[x^*,y^*]$:

$$\delta x=x-x^*,$$
$$\delta y=y-y^*.$$

The corresponding linearised reaction-diffusion system is

$$\frac{\partial}{\partial t}\begin{bmatrix}\delta x\\ \delta y\end{bmatrix}=\Psi\frac{\partial^2}{\partial r^2}\begin{bmatrix}\delta x\\ \delta y\end{bmatrix}+DF(X^*)\begin{bmatrix}\delta x\\ \delta y\end{bmatrix} \tag{27}$$

where δx and δy are displacements from the steady states $X^*=[x^*,\ y^*]^T$ and are dependent on both time and space. $DF(X^*)$ is the Jacobian matrix evaluated at the steady state X^*. The matrix $\Psi=\begin{bmatrix}1 & 0\\ 0 & \psi_y\end{bmatrix}$ contains diffusion constants for the spatio-temporal model. We determined the stability of the homogeneous steady states against small perturbations considering both time and spatial effects.

Suppose that the perturbations are inhomogeneous in space and since Equation (27) is linear, we can seek a particular solution which has a convenient form that can be given as:

$$\begin{bmatrix}\delta x\\ \delta y\end{bmatrix}=\begin{bmatrix}\delta x_0\\ \delta y_0\end{bmatrix}e^{\lambda_k t}e^{ikr}, \tag{28}$$

where λ_k is the eigenvalue which determines the temporal growth rate. The spatial variation is assumed to be $e^{ikr} = \cos(kr) + i\sin(kr)$ and corresponds to the wave number k. We choose $e^{\lambda_k t}$ to be the temporal variation to allow the perturbations to grow, diminish, or oscillate. Both δx_0 and δy_0 have similar dependence on time and space and they are components of the perturbation vector $[\delta x,\ \delta y]^T$. Substituting Equation (28) into (27) and cancelling off the common exponentials yields the following linearized reaction-diffusion system:

$$\lambda_k \begin{bmatrix} \delta x_0 \\ \delta y_0 \end{bmatrix} = \begin{bmatrix} -k^2 & 0 \\ 0 & -k^2\Psi_y \end{bmatrix} \begin{bmatrix} \delta x_0 \\ \delta y_0 \end{bmatrix} + D\boldsymbol{F}(\boldsymbol{X}^*) \begin{bmatrix} \delta x_0 \\ \delta y_0 \end{bmatrix}. \tag{29}$$

Rearranging we have

$$\left\{\lambda_k \mathrm{I} + k^2\Psi - D\boldsymbol{F}(\boldsymbol{X}^*)\right\} \begin{bmatrix} \delta x_0 \\ \delta y_0 \end{bmatrix} = 0,$$

where I is the identity matrix. This is a homogeneous equation in $[\delta x_0\ \delta y_0]$ which has non trivial solutions only if the determinant,

$$\left|\lambda_k \mathrm{I} + k^2\Psi - D\boldsymbol{F}(\boldsymbol{X}^*)\right| = 0.$$

The diffusion constants for the immune cells Ψ_X and tumour cells Ψ_Y are equal. Hence, the diffusion ratio Ψ_y equals 1. Stability analysis involves evaluating the new Jacobian matrix at the homogeneous steady states.

Theorem 4.3. *There is a possibility of a diffusion induced stability of the tumour free state if* $k^2 > \sigma\frac{\nu_2}{\psi_2}$.

Proof of Theorem 4.3. Evaluating the Jacobian matrix at the tumour free state X_2^*, one obtains

$$\lambda_k \begin{bmatrix} \delta x_0 \\ \delta y_0 \end{bmatrix} = \begin{bmatrix} -k^2 - \psi_1 & \frac{\delta}{\psi_2\gamma} + \frac{\nu_1}{\psi_2} \\ 0 & -k^2 - \left(\sigma_1 - \frac{\nu_2}{\psi_2}\right) \end{bmatrix} \begin{bmatrix} \delta x_0 \\ \delta y_0 \end{bmatrix}$$

The eigenvalues for the tumour free steady state are:

$$-k^2 - \psi_1 \ \text{ and } \ -k^2 - \left(\sigma_1 - \frac{\nu_2}{\psi_2}\right).$$

Dynamical stabilization is likely to be observed for the unstable tumour-free steady state if and only if $k^2 > \left(\sigma_1 - \frac{\nu_2}{\psi_2}\right)$. Otherwise, it is an unstable saddle point. The stabilization of the tumour-free steady state depends on the wave number. This means that there is a possibility of achieving a tumour-free state for sometime though this state might not last for a very long time and the tumour cells may reoccur. □

The tumour dormant state involves huge expressions and determining its stability is not an easy undertaking. Non-dimensional parameter values in non-dimensional in Equation (31) are therefore used. Evaluating the Jacobian matrix at the tumour-dormant steady state X_4^* gives:

$$\lambda_k \begin{bmatrix} \delta x_0 \\ \delta y_0 \end{bmatrix} = \underbrace{\begin{bmatrix} -k^2 - 5.8062 & 4.6405 \\ -0.2689 & -k^2 - 0.7174 \end{bmatrix}}_{D\boldsymbol{F}(\boldsymbol{X}_4^*)} \begin{bmatrix} \delta x_0 \\ \delta y_0 \end{bmatrix}.$$

One of the signs of the off-diagonal entries in the Jacobian matrix are not opposite as required by Turing instability. Therefore, in this case diffusion does not have a destabilizing effect on the globally stable tumour-dormant steady state. Moreover, the trace

and determinant of the Jacobian matrix indicate that the eigenvalues are always negative.

$$tr(D\boldsymbol{F}(\boldsymbol{X}_4^*)) = -2k^2 - 6.5236 < 0,$$
$$det(D\boldsymbol{F}(\boldsymbol{X}_4^*)) = k^4 + 6.5236k^2 + 4.1654 > 0.$$

The trace is always negative and the only way diffusion could destabilize the system is when the determinant becomes negative. This means that the random movement of tumour and immune cells does not destabilise the tumour-dormant state. This could as well explain why some people can have a dormant tumour for their entire lifetime. Next, Equations (7) are numerically simulated.

5. **Numerical simulations.** In this section, numerical simulations of both the temporal and spatiotemporal models are determined. Estimated parameter values were obtained from Chaplian *et al.* [51], Hahnfeldt [52] and Matzavinos *et al.* [18]. Their estimates, descriptions and numerical values are stated in Table 1.

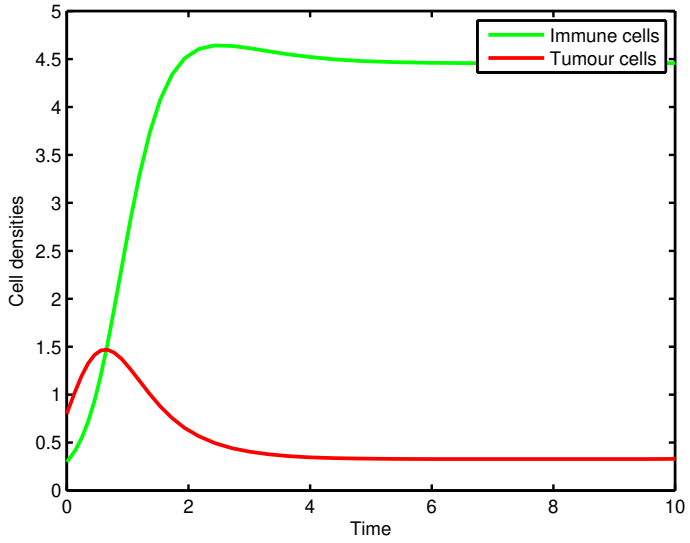

FIGURE 2. **A plot of cell densities with time for non-dimensional parameter values in Equation (30) and $x_0 = 0.3$, $y_0 = 0.8$, $u_0 = 10^{-6}$, $y^* = 0.1$ and $R_0 = 0.8$. The simulations show the cell densities settling at a stable tumour dormant state. One density unit is equivalent to 10^6 cells cm $^{-3}$ and 1 unit of time is equivalent to 24 days.**

5.1. **Homogeneous simulations.** We present numerical simulations of the model Equations (11) to predict changes in tumour size in response to the immune response. The *ode23s* [53], a stiff ODE solver, in *Matlab*© is used to integrate the equations. The initial tumour, immune and chemokine densities are respectively considered to be $X_0 = 10^6$, $Y_0 = 10^7$ and $U_0 = 10^{-10}$ cells per unit volume [18] and the initial tumour radius is taken to be $R_0 = 0.1$ cm. 1% of the initial tumour density is considered to be dead, that is $Y_0^* = 10^5$ cells per unit volume. In rescaling the model, time is rescaled relative to the

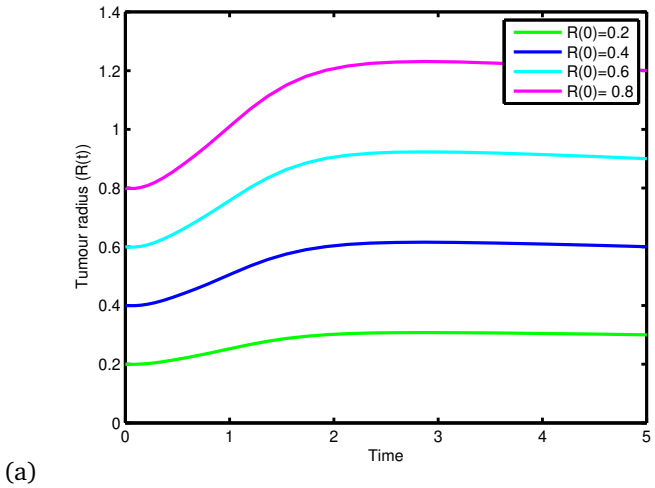

(a)

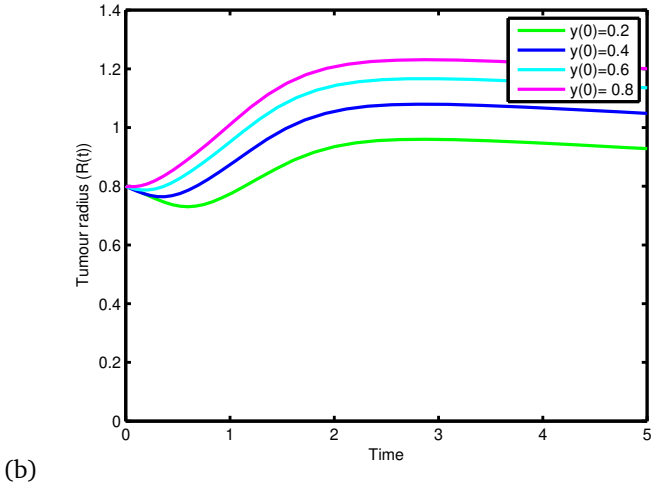

(b)

FIGURE 3. **A plot of tumour radius against time (a) with different initial radii and (b) with different initial tumour densities. The simulations show the tumour radius increasing with increasing initial tumour radius and initial tumour cell density.**

rate of chemokine decay, that is, $t_0 = d_1^{-1}$. One density unit is equivalent to 10^6 cells cm $^{-3}$ and 1 unit of time is equivalent to 24 days and the following non-dimensional parameter values in Equation (30) are used in doing all the temporal model simulations.

$$\begin{aligned} &\varphi_1 = 1.3398,\ \varphi_2 = 0.25,\ \delta = 3.0218,\ \nu_1 = 0.00218,\ \sigma_1 = 3.8835,\ \sigma_2 = 0.5,\\ &\nu_2 = 0.7279,\ \nu_3 = 300,\ \mu_1 = 1,\ \rho = 0.1,\ \mu_2 = 0.24. \end{aligned} \tag{30}$$

Figure 2 shows that the tumour cells reduce by half as a result of the interactions between tumour cells with immune cells. The tumour cells decrease by approximately 62% from an initial concentration of 0.8 to 0.3 as a result of its interaction with immune cells instead of growing to their carrying capacity. Unfortunately, tumour cells are not

completely eliminated from the host's body but are rather reduced to a dormant lower concentration.

Figure 3 is a numerical representation of the tumour radius with time for different initial tumour radii and tumour densities. The figure shows that the radius, generally, increases to a dormant state. It is important to note that without tumour immune interactions, the tumour density would rise to its carrying capacity and the tumour radius would exponentially grow. Both Figures 3 (a) and (b) respectively show that increasing the initial tumour radius and initial tumour density leads to an increase in the tumour radius.

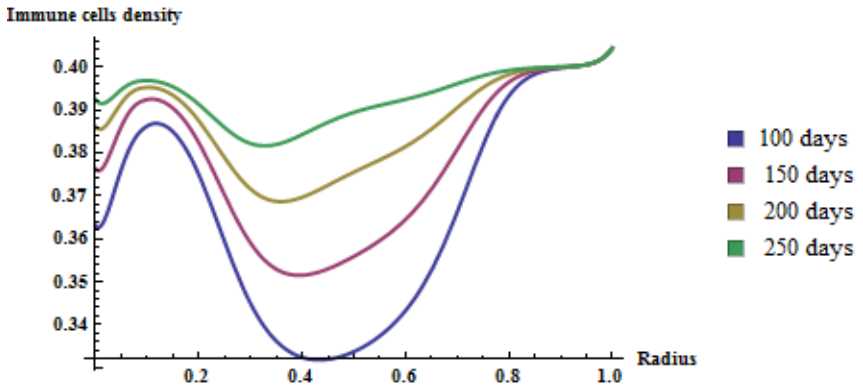

FIGURE 4. **Spatio-temporal distribution of immune cells after 100, 150, 200 and 250 days respectively. The immune cell density increases to its carrying capacity with time. One density unit is equivalent to 10^6 cells cm $^{-3}$ and 1 unit of time is equivalent to 100 days.**

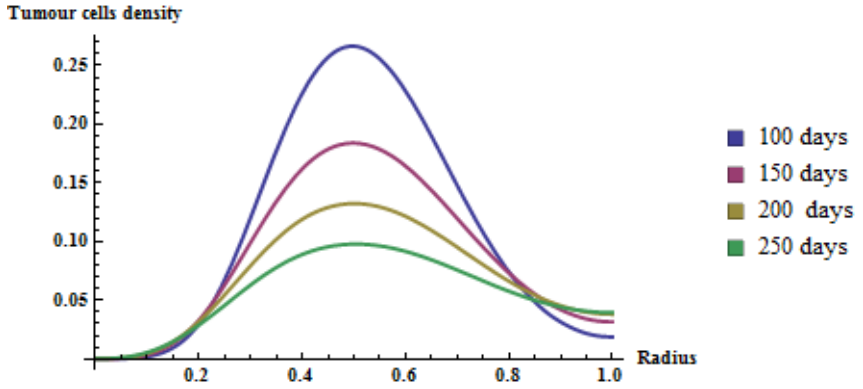

FIGURE 5. **Spatio-temporal distribution of tumour cells corresponding to 100, 150, 200 and 250 days respectively. The tumour cell density reduces with time. One density unit is equivalent to 10^6 cells cm $^{-3}$ and 1 unit of time is equivalent to 100 days.**

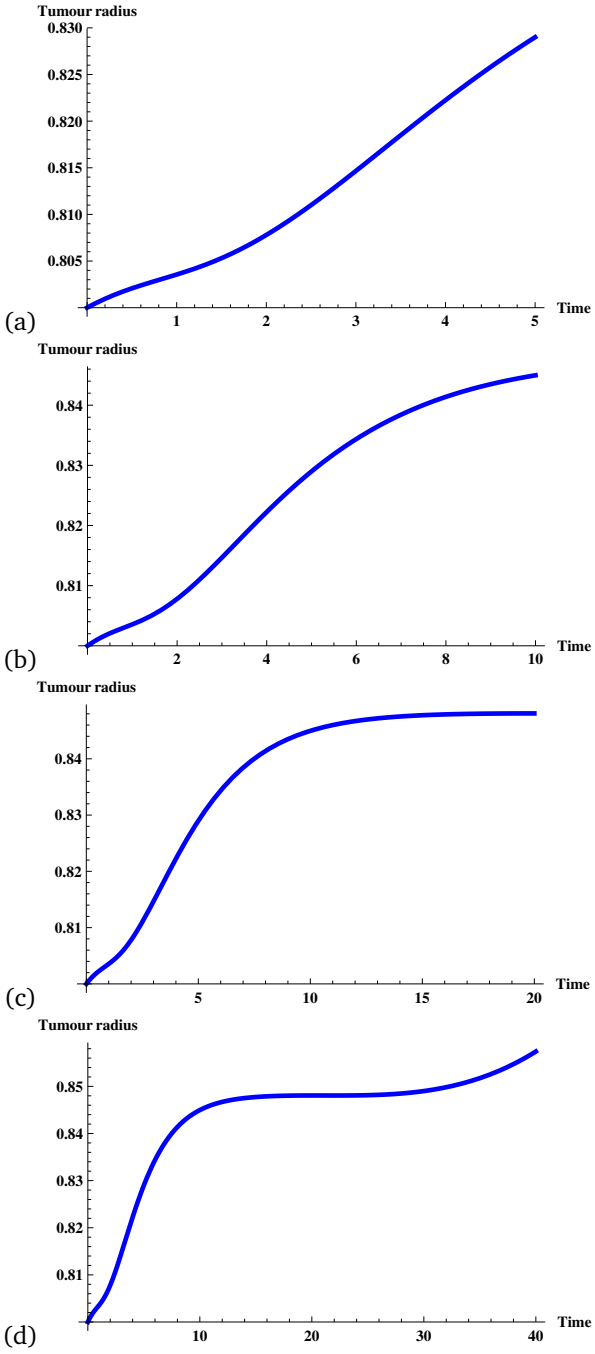

FIGURE 6. **Tumour radius against time after (a) 500, (b) 1000 (c) 2000 days and (d) 4000 days respectively. The tumour swells to a dormant state.**

5.2. **Spatio-temporal model simulations.** We now present numerical simulations of the moving boundary problem (7) to investigate tumour-immune interactions in a spherical geometric setting under the assumption of radial symmetry. The method of lines

(MOL) in *Mathematica*© [54], that is NDSolve, is used to integrate the equations. The initial tumour, immune and chemokine concentrations are respectively taken to be $X_0 = 10^6$, $Y_0 = 10^7$ and $U_0 = 10^{-10}$ cells per unit volume [18]. The initial tumour radius is assumed to be 0.1 cm and 1% of the initial tumour density is considered to be dead, that is $Y_0^* = 10^5$ cells per unit volume. In rescaling we take $t_0 = d_2^{-1}$ which gives rise to the following non-dimensional parameter values:

$$\begin{aligned} &\psi_x = \psi_y = \beta = 0.01, \quad \varphi_1 = 22, \quad \varphi_2 = 2.5, \quad \gamma = 202, \quad \nu_1 = 0.00009, \quad \nu_2 = 1 \\ &\sigma_1 = 0.016, \quad \sigma_2 = 50, \quad \nu_3 = 30000, \quad \mu_1 = 4.17 \times 10^{-12}, \quad \rho = 0.1. \end{aligned} \tag{31}$$

The non-dimensional parameter values in Equation (31) were used in all spatio-temporal model simulations unless stated otherwise. Figure 4 shows the spatio-temporal distribution of immune cells after 100, 150, 200 and 250 days respectively. The figure shows that the immune density increases with time. For example after the 10th day, the density had risen from 0.3×10^6 to about $0.36 - 0.39 \times 10^6$ cells per unit volume. The immune cells re-distribute to occupy more of the regions $0.1 \leq r \leq 0.3$ and $0.7 \leq r \leq 1$.

Figure 5 is a spatio-temporal representation of tumour cells after 100, 150, 200 and 250 days respectively. The figure depicts the tumour density reducing with time for example after 250 days, the density had dropped from 0.8×10^6, its initial value, to approximately 0.1×10^6 cells per unit volume. The region in which the tumour cells occupy slightly widens.

Figure 6 shows the moving boundary. It is a plot of the tumour radius with time after 500, 1000, 2000 and 4000 days respectively. The figure depicts that tumour radius increasing to a dormant state. Nonetheless, figure 6(d) depicts that the radius may begin to increase after about 8.2 years (3000 days).

6. **Conclusion.** The primary role of the immune system is to defend and protect the body from invading pathogens such as viruses, bacteria, fungi, or in some cases, cells in the body that may become cancerous [7–9, 55]. The mechanisms of tumour-immune interactions are however not fully understood. A full characterisation of these interactions can lead to the development of more efficient cancer therapies [3, 16]. In an attempt to extend previous studies on the growth dynamics of tumour cells in the presence of an immune response, we developed a mathematical model in the form of a moving boundary problem. The model describes the growth of an avascular tumour, in a spherically goemetric setting under radial symmetry, with a time dependent radius.

The main aim in this article was to give further insights on tumour-immune interactions by keeping track of the tumour radius with time, examining critical parameters that promote cancer dormancy and analysing the spatial distribution associated with an immune response to the presence of cancer cells. Analysis of the temporal model included studying the model phase properties, determining asymptotic solutions and analysing their stability. The spatio-temporal model was analysed by determining analytical travelling wave solutions, calculating their minimum wave speeds and investigating the effect of diffusion on the homogeneous steady states. Numerical experiments of both temporal and spatiotemporal models were done using data from clinical experiments on dormant tumours *in vitro*.

Analysis of the temporal model in Section 3 revealed that there exists a globally stable tumour dormant state for certain parameter sets for example those in Table 1. This could perhaps be proof as to why someone can live with a dormant tumour for ages [4, 5]. Further, it was shown that a tumour free steady state may be achieved only if intrinsic tumour growth rate is less than the immune strength. This condition points

out that any cancer treatment should seek to reduce the tumour growth rate, increase the tumour induced death by immune cells and increase their carrying capacity.

The travelling wave solutions which we determined in Equations (20) & (21) together with their minimum wave speeds in Equation (22) were characterized by the cell growth rates and diffusivity. This suggests that the cell invasion dynamics are mainly driven by their motion and growth rates. Treatment options should indeed strive to improve immune recognition of tumour cells, reduce the intrinsic growth rate of tumour cells and increase that for immune cells. Immune cell growth rate can probably be increased by boosting the immune system and tumour growth can be curtailed by producing effective drugs. Turing instability analysis showed that diffusion does not have a destabilizing effect on both of the homogeneous states. This could also possibly explain why one can live with a dormant tumour for many years.

Numerical simulations of the temporal model in Section 5 showed the cell concentrations stabilising at a stable dormant state. The tumour radius was also found to increase to a dormant level. The tumour radius plots in Figure 6 showed the tumour swelling to a dormant state although it would regrow after several years. This result is in line with clinical evidence that some people have lived with a benign tumour for a long period of time with relapse 5-25 years later. Moreover this condition is common in patients with breast cancer, cell lymphoma, and melanoma [3]. The results in this study may lead to a deeper understanding of cancer dormancy and this may be helpful in the future development of better and effective therapeutic methods.

Appendix.

Parameter estimation. The kinetic parameters in Table 1 are estimated from clinical experiments of dormant tumours *in vitro*. The estimates are obtained from Chaplain *et al*. [51] and Wilkie & Hahnfeldt [52]. These values are taken from experimental data on Marine B cell lymphoma (BCL_1). BCL_1 lymphomas are considered to be very good for *in vivo* experimental models given that the tumour cells are spatially contained within the lymph tissue of the spleen. The diffusion and chemotaxis constants are obtained from Matzavinos *et al*. [18]. Table 1 gives a summary of the dimensional parameter descriptions together with their values and units of measurements.

TABLE 1. **A summary of the dimensional parameters with their values and units. All obtained or derived from Chaplian *et al.* [51], Hahnfeldt [52] and Matzavinos *et al.* [18].**

Parameter	Description	Value	Unit of measure
ψ_X	Immune cells' diffusivity	10^{-6}	$\text{cm}^3\ \text{day}^{-1}$
ψ_Y	Tumour cells' diffusivity	10^{-6}	$\text{cm}^3\ \text{day}^{-1}$
ψ_U	Chemokine diffusivity	$0.6 - 9 \times 10^{-6}$	$\text{cm}^3\ \text{day}^{-1}$
β	Chemotaxis constant	1.728×10^6	$\text{day}^{-1}\ \text{moles}^{-1}\text{cells} \cdot \text{cm}^{-3}$
α_1	Intrinsic growth rate of immune cells	0.22	day^{-1}
α_2	Inverse carrying capacity of immune cells	2.5×10^{-7}	$\text{cells}^{-3}\ \text{cm}^3$
β_1	Intrinsic growth rate of tumour cells	0.16	day^{-1}
β_2	Inverse carrying capacity of tumour cells	5×10^{-5}	$\text{cells}^{-3}\ \text{cm}^3$
f	Immune cells' proliferation rate	0.2988×10^8	$\text{day}^{-1}\text{cells} \cdot \text{cm}^3$
γ	Michaelis-Menten constant	2.02×10^7	$\text{cells} \cdot \text{cm}^{-3}$
k_1	Immune cells' binding rate to tumour cells	1.3×10^{-7}	day^{-1}
k_2	Immune cells' detachment rate	7.2	day^{-1}
k_{-1}	Tumour cells' detachment rate	24	day^{-1}
d_1	Rate of decay of chemokine concentration	0.0417	day^{-1}
d_2	Rate of decay of dead immune cells	0.01	day^{-1}
d_3	Rate of decay of dead tumour cells	0.01	day^{-1}
ϕ_1	Immune cell deactivation rate rate	9×10^{-11}	$\text{cells} \cdot \text{cm}^{-3}\text{day}^{-1}$
ϕ_2	Tumour cell deactivation rate	3×10^{-8}	$\text{cells} \cdot \text{cm}^{-3}\text{day}^{-1}$
ϕ_3	Chemokine production rate	3×10^{-6}	$\text{cells} \cdot \text{cm}^{-3}\text{day}^{-1}$

$\phi_1 = \frac{k_1 k_2 (1-p)}{k_{-1}+k_2}$, $\phi_2 = \frac{k_1 k_2 p}{k_{-1}+k_2}$.

References

[1] J. Dittmer. Mechanisms governing metastatic dormancy in breast cancer. *In Seminars in Cancer Biology. Academic Press*, doi:10.1016/j.semcancer.2017.03.006

[2] G. Pukazhendhi and S. Gluck Circulating tumor cells in breast cancer. *Carcinogenesis*, 13(1):p.8, 2014. doi:10.4103/1477-3163.135578

[3] J. W. Uhr and Pantel, k. Pantel Controversies in clinical cancer dormancy. *Proceedings of the National Academy of Sciences*, 108(30):12396–12400, 2011. doi:10.1073/pnas.1106613108.

[4] J. A. Aguirre-Ghiso Models, mechanisms and clinical evidence for cancer dormancy. In *Nature Reviews Cancer*, volume 7(11), pages 834–846. Elsevier, 2007.

[5] M. S. Sosa, P. Bragado and J. A. Aguirre-Ghiso Mechanisms of disseminated cancer cell dormancy: an awakening field. *Nature Reviews Cancer*, 14(9):611–622, 2014. doi:10.1038/nrc3793

[6] P. Parham. How the immune system works. John Wiley and Sons, 2015

[7] E. Hoe, J. Anderson, and J. Nathanielsz, and Z. Q. Toh, and R. Marimla, and A. Balloch, and P. V. Licciardi. The contrasting role of Th17 immunity in human health and disease. *Microbiology and Immunology*, 2017. doi:10.1111/1348-0421.12471

[8] V. Hořejší. Antitumour Weapons of the Immune System. *Klinicka onkologie: casopis Ceske a Slovenske onkologicke spolecnosti*, 28:4S15–22, 2017.

[9] w. Deng, B.G. Gowen, L. Zhang, L. Wang, S. Lau, A. Iannello, ... and D. H. Raulet. A shed NKG2D ligand that promotes natural killer cell activation and tumor rejection. *Cellular Immunology*, 348(6230):136–139, 2015. doi:10.1126/science.1258867.Epub2015Mar5

[10] M. Chaplain and A. Matzavinos. Mathematical modelling of spatio-temporal phenomena in tumour immunology. In Tutorials in Mathematical Biosciences III. (pp. 131-183). Springer Berlin Heidelberg 2006.

[11] K. M. Wilson and EM Lord. Specific (emt6) and non-specific (wehi-164) cytolytic activity by host cells infiltrating tumour spheroids. *British Journal of Cancer*, 55(2):141, 1987.

[12] S. M. Dubinett, J. Lee, s. Sharma, and J. J. Mulé. Chemokines: can effector cells be re-directed to the site of tumor?. *Cancer Journal (Sudbury, Mass.)*, 16(4):235, 2010. doi:10.1097/PPO.0b013e3181eb33bc

[13] G. A. Duque, Guillermo and A. Descoteaux Macrophage cytokines: involvement in immunity and infectious diseases. *Secretion of Cytokines and Chemokines by Innate Immune Cells*, 6, 2015. doi:10.3389/fimmu.2014.00491

[14] B. Quesnel Dormant tumor cells as a therapeutic target. *Cancer Letters*, 267(1):10–17, 2008. http://dx.doi.org/10.1016/j.canlet.2008.02.055

[15] C. G. Ioannides and T. L. Whiteside. T cell recognition of human tumors: implications for molecular immunotherapy of cancer. *Clinical Immunology and Immunopathology*, 66(2):91–106, 1993.

[16] T. F. Gajewski. Failure at the effector phase: immune barriers at the level of the melanoma tumor microenvironment. *Clinical Cancer Research*, 13(18):5256–5261, 2007. http://DOI:10.1158/1078-0432.CCR-07-0892

[17] T. Udagawa. Tumor dormancy of primary and secondary cancers. *Apmis*, 116(7-8):615–628, 2008. DOI:10.1111/j.1600-0463.2008.01077.x

[18] A. Matzavinos, M. A. J. Chaplain, and V. A. Kuznetsov. Mathematical modelling of the spatio-temporal response of cytotoxic T-lymphocytes to a solid tumour. *Mathematical Medicine and Biology*, 21(1):1–34, 2004.

[19] A. Eladdadi, P. Kim and D Mallet. Mathematical models of tumor-immune system dynamics. Springer, 2014.

[20] K. Page and J. Uhr Mathematical models of cancer dormancy. *Leukemia and lymphoma*, 46(3):313–327, 2005. http://DOI:10.1080/10428190400011625

[21] D. G. Mallet, and L. G. De Pillis. A cellular automata model of tumor–immune system interactions. *Theoretical Biology*, 239:(3), 334–350, 2006.http://dx.doi.org/10.1016/j.jtbi.2005.08.002

[22] L. G. de Pillis, D. G. Mallet, and E. A. Radunskaya. Spatial tumor-immune modeling. *Computational and Mathematical Methods in Medicine*, 7:(2–3), 159–176, 2006.http://dx.doi.org/10.1080/10273660600968978

[23] A. d'Onofrio, u. Ledzewicz, and H. Schättler. On the dynamics of tumor-immune system interactions and combined chemo-and immunotherapy. In *New challenges for cancer systems biomedicine* 249–266, 2012.

[24] K. P. Wilkie, and P. Hahnfeldt. Mathematical models of immune-induced cancer dormancy and the emergence of immune evasion. *Interface Focus*, 3(4):20130010, 2013. DOI:10.1098/rsfs.2013.0010

[25] H. Mambili-Mamboundou, P. Sibanda, and J. Malinzi. Effect of immunotherapy on the response of TICLs to solid tumour invasion. *Mathematical Biosciences*, 249:52–59, 2014.http://dx.doi.org/10.1016/j.mbs.2014.01.002

[26] G. Caravagna, A. d'Onofrio, P. Milazzo, R. Barbuti. Antitumor immune surveillance through stochastic oscillations. *Theoretical Biology*, 265:(3) 336–345, 2010.

[27] A. d'Onofrio. Bounded-noise-induced transitions in a tumor-immune system interplay. *Physical Review E*, 81:(2) 021923, 2010.DOI:10.1103/PhysRevE.81.021923

[28] P. Cattiaux, C. Christophe and S. Gadat. A stochastic model for Cytotoxic T. Lymphocyte interaction with tumor nodules. *Journal of Mathematical Biology*, 2:(5) 2016.

[29] N. Bellomo and M. Delitala. From the mathematical kinetic, and stochastic game theory to modelling mutations, onset, progression and immune competition of cancer cells. *Physics of Life Reviews*, 5:(4) 183–206, 2008. http://dx.doi.org/10.1016/j.plrev.2008.07.001

[30] K. M. Page. Mathematical Modelling of Tumour Dormancy. *Mathematical Modelling of Natural Phenomena*, 4(3):68–96, 2009. https://doi.org/10.1051/mmnp/20094303

[31] R. Eftimie, and J. L. Bramson, and D. J. D. Earn Interactions between the immune system and cancer: a brief review of non-spatial mathematical models. In *Bulletin of Mathematical Biology* 2–32, 73 (1), 2011. doi:10.1007/s11538-010-9526-3

[32] P. K. Wilkie. A review of mathematical models of cancer–immune interactions in the context of tumor dormancy. In *Systems Biology of Tumor Dormancy* 201–234, Springer, 2013. 10.1007/978-1-4614-1445-2_10

[33] H. P. Greenspan. Models for the growth of a solid tumor by diffusion. *Studies in Applied Mathematics*, 51 (4):317–340, 1972. DOI:10.1002/sapm1972514317

[34] A. Friedman. A hierarchy of cancer models and their mathematical challenges. *Discrete and Continuous Dynamical Systems Series B*, 4(1):147–160, 2004. DOI:10.3934/dcdsb.2004.4.147

[35] H. M. Byrne. Mathematical Biomedicine and modeling avascular tumor growth. University of Oxford, 2012.

[36] L. Michaelis and M. L. Menten. Die kinetik der invertinwirkung. *Biochem. z*, 49(1):333-369, 1913.

[37] L. Michaelis, M. L. Menten, K. A. Johnson and R. S. Goody. The original Michaelis constant: translation of the 1913 Michaelis-Menten paper. Biochemistry, 50(39):8264, 2011. doi:10.1021/bi201284u

[38] V. A. Kuznetsov, I. A. Makalkin, M. A. Taylor, and A. S. Perelson. Nonlinear dynamics of immunogenic tumors: parameter estimation and global bifurcation analysis. *Bulletin of Mathematical Biology*, 56(2): 295–321, 1994.

[39] J. G. Wagner. Properties of the Michaelis-Menten equation and its integrated form which are useful in pharmacokinetics. *Pharmacokinetics and Biopharmaceutics*, 1(2):103–121, 1973.

[40] A. H. Kyle, C. T. O. Chan, and A. I. Minchinton. Characterization of three-dimensional tissue cultures using electrical impedance spectroscopy. *Biophysical Journal*, 76(5):2640–2648, 1999. http://dx.doi.org/10.1016/S0006-3495(99)77416-3

[41] L. G. De Pillis and A. Radunskaya. A mathematical tumor model with immune resistance and drug therapy: an optimal control approach. *Computational and Mathematical Methods in Medicine*, 3(2):79–100, 2001. http://dx.doi.org/10.1080/10273660108833067

[42] E. Özuğurlu. A note on the numerical approach for the reaction–diffusion problem to model the density of the tumour growth dynamics. *Computers and Mathematics with Applications* ,**69(12)** (2015):1504–1517. DOI:10.1016/j.camwa.2015.04.018

[43] M. A. J. Chaplain and G. Lolas. Mathematical modelling of cancer invasion of tissue: dynamic heterogeneity. *Networks and Heterogeneous Media*,**1(3)** (2006):399–439. doi:10.3934/nhm.2006.1.399

[44] H.G.Landau. Heat conduction in a melting solid. *The Quartely Journal of Mechanics and Applied Mathematics*,(8):81–94, 1950.

[45] H. R. Thieme. Mathematics in population biology. Princeton University Press, 2003.

[46] W. Malfliet, *The tanh method: a tool for solving certain classes of nonlinear evolution and wave equations*, Computational and Applied Mathematics, **164** (2004), 529–541, doi:http://dx.doi.org/10.1016/S0377-0427(03)00645-9.

[47] W. Malfliet, *Solitary wave solutions of nonlinear wave equations*, American Journal of Physics, **60(7)** (1992), 650–654, doi:http://dx.doi.org/10.1119/1.17120.

[48] W. Malfliet and W. Hereman, *The tanh method: I. Exact solutions of nonlinear evolution and wave equations*, Physica Scripta, **54(6)** (1996), 563, doi:http://iopscience.iop.org/article/10.1088/0031-8949/54/6/003/meta.

[49] A. M. Turing. The chemical basis of morphogenesis. *Philosophical Transactions of the Royal Society of London B: Biological Sciences*, 237(641):37–72, 1952.

[50] J. Shi, Z. Xie, and K. Little. Cross-diffusion induced instability and stability in reaction-diffusion systems. *Journal of Applied Analysis and Computation* , 1(1):95–119, 2011.
[51] M. Chaplain, V. A. Kuznetsov, Z. H. James, and L. A. Stepanova. Spatio-temporal dynamics of the immune system response to cancer. In *Paper presented at the 1997' International Conference on Mathematical Models in Medical and Health Sciences' Nashville, 28th-31st May 1997*. Vanderbilt University Press, 1998.
[52] K. P. Wilkie and P. Hahnfeldt. Tumor–immune dynamics regulated in the microenvironment inform the transient nature of immune-induced tumor dormancy. *Cancer Research*, 73(12):3534–3544, 2013. doi: 10.1158/0008-5472.CAN-12-4590
[53] R. Knapp. A method of lines framework in mathematic. *Numerical Analysis, Industrial and Applied Mathematics*,**318(1)** (2008):43–54.
[54] L. F. Shampine and M. W. Reichelt. The matlab ode suite. SIAM journal on scientific computing. *SIAM Journal of Scientific Computing*,**18(1)**(1997):1-22.
[55] PubMed Health, The innate and adaptive immune systems https://www.ncbi.nlm.nih.gov/pubmedhealth/PMH0072580/, 02-04-2017.

E-mail address: josephmalinzi1@gmail.com
E-mail address: innocenter@aims.ac.za